



## ANTIMICROBIAL AND *IN VITRO* CYTOTOXICITY EFFECT OF GREEN SYNTHESIZED SILVER NANOPARTICLES USING AQUEOUS LEAF EXTRACT OF *SENNA HIRSUTA*

Narahari N. Palei<sup>1\*</sup>, M.P. Bhuvana<sup>2</sup>, R. Jayaraman<sup>3</sup> and Arghya Kusum Dhar<sup>4</sup>

<sup>1</sup>Amity Institute of Pharmacy, Amity University Uttar Pradesh, Lucknow Campus, India

<sup>2</sup>Sree Vidyanikethan College of Pharmacy, Tirupati, Andhra Pradesh, India

<sup>3</sup>Shri Venkateshwara College of Pharmacy, Ariyur, Pondicherry, India

<sup>4</sup>School of Pharmacy, The Neotia University, Sarisha, West Bengal, India

*In this study, we prepared silver nanoparticles (AgNPs) using an aqueous Senna hirsuta leaf extract. The AgNPs were characterized using UV visible spectrophotometer, particle size, zeta potential, energy diffraction X-ray (EDAX), Fourier transform infrared (FTIR), transmission electron microscopy (TEM) and determined antibacterial and cytotoxicity impact of the AgNPs. UV-Visible spectroscopy of Senna hirsuta leaf extract synthesized into AgNPs was carried out at various time intervals. The peak ( $\lambda$  max) was observed at 436–446 nm and it was broad. The particle size of the synthesized AgNPs was found 28.3 nm. The Zeta potential of AgNPs was found -4.4 mV. TEM analysis demonstrated that nanoparticles have a spherical form. According to the EDAX analysis, the extract effectively capped the AgNPs. Zone of inhibition of AgNPs were observed more than those of the extract. Silver nanoparticles demonstrated effective antimicrobial activity due to their large surface area, which allows for stronger contact with cell wall of bacteria. In vitro cytotoxicity showed that synthesized AgNPs a prominent cytotoxicity activity against MCF7 cell lines.*

**Keywords:** Green synthesis, Senna hirsuta, Silver nanoparticles, Antimicrobial activity, Cytotoxicity

### INTRODUCTION

Recently, conventional antimicrobial agents have been ineffective due to resistance developed by microorganisms and most of the effective agents are highly toxic making them less applicable. Owing to frequent infectious disease outbreaks caused by different types of microorganisms and the development of antibiotic resistance, pharmaceutical companies are in search of new antibacterial agents. Antibacterial applications of nanotechnology are gaining its prominence to prevent unpredictable consequences of antibiotic resistance. The use of metal and metal oxide nanoparticles to kill bacteria as a substitute for antibiotics has recently gained attention. A new front in the fight against the spread of infectious illnesses has been generated by the

combination of biosynthesis and nanotechnology, which has created materials on nano scale<sup>1</sup>. The development of nanomaterials with size-dependent characteristics is an exciting field of nanoparticles research. Gold, silver, and copper are just few of the metallic nanomaterials studied; however, silver nanoparticles (AgNPs) have proven to be the most effective due to their better antibacterial and cytotoxicity activity<sup>2</sup>. Due to its appealing physicochemical features AgNPs play a crucial role in the fields of medicine and biology<sup>3&4</sup>. Wound healing<sup>5&6</sup>, endodontic treatment<sup>7</sup>, treatment of burn infection<sup>8</sup>, treatment of epilepsy<sup>9</sup> and development of medical devices<sup>10</sup> are some of the medicinal applications for silver nanoparticles. AgNPs are also one of the widely explored metal nanoparticles, which

showed efficient cytotoxicity effect against various types of cancer cells<sup>11</sup>. Various works are reported the cytotoxicity potential of silver nanoparticles against MCF7 breast cancer cell lines<sup>12&13</sup>. Chemical reduction<sup>14</sup>, photochemical<sup>15</sup>, electrochemical<sup>16&17</sup>, physical and biological approaches<sup>18</sup> are mostly used to produce silver nanoparticles. Biological microorganisms like bacteria<sup>19</sup>, plant extracts<sup>20,21</sup>, and fungus<sup>22</sup> have all been used in the production of silver nanoparticles. Biosynthetic nanoparticles have been developed as a simple replacement for chemical nanoparticles synthesis. Since it is cost-effective and environmentally friendly, green synthesis has quickly become the industry standard. Nanoparticles for green synthesis can be prepared by interacting together metals and plant extracts. In green synthesis, there is no need to use any chemicals that are hazardous to reducing metals because plant extracts itself act as reducing agents and capping agent. Nanoparticles synthesis using microorganisms like bacteria and fungus is also possible, but the reaction rate is much slower than with green synthesis<sup>23</sup>. In order to reduce metal to nanoparticles, physical and chemical processes typically include the use of chemical compounds, which cause some risks to human health. The nanoparticles preparation from plant extracts is sensitive to variables like reaction duration, pH, and temperature. *Senna hirsuta* is a large, upright herbaceous plant or (perennial) shrub that grows between 0.5 and 3 meters in height and becomes slightly woody with age. Long, silvery white hair coats every inch of the plant's stems, leaves, and pods. It is a common weed in the tropics of South and Southeast Asia and elsewhere in the old world. These leaves contain a wide variety of chemical compounds, including saponins, tannins, alkaloids, flavonoids, and anthraquinones. In this study, we have synthesized silver nanoparticles (AgNPs) using *Senna hirsuta* leaf extract for antimicrobial and *in vitro* cytotoxicity effect against MCF 7 cell lines.

## MATERIALS AND METHODS

### Materials

Silver nitrate (AgNO<sub>3</sub>), and Agar were procured from Himedia, Mumbai. 3-(4,

5dimethylthiazol-2-yl)-2, 5-diphenyl tetrazolium bromide (MTT) were procured from Sigma-aldrich, Bangalore. Dimethyl Sulfoxide (DMSO) was procured from Himedia, Mumbai. Streptomycin was purchased from Yarrow Chem, India. All other chemicals used in the study were of an analytical grade.

### Leaves Collection and extract preparation

*Senna hirsuta* leaves were collected from the local area of Tirupathi, Andhra Pradesh and cleaned in running water before use. The plant extract was obtained during the hot maceration process. Fifty grams of washed leaves were kept in a beaker and 50 mL of distilled water was added and boiled in a water bath for 30 min. The temperature range was maintained between 40 and 50 °C. The extract was cooled down and the resulting solution was filtered using Whatman filter paper before being placed in the refrigerator for later use.

### Phytochemical screening

Phytochemical screening was performed on *Senna hirsuta* leaf extract to identify the presence of phytoconstituents. Reducing sugars (Fehling's test), terpenoids (Salkowski's test), flavonoids (Shinoda's test), phenolic compounds (ferric chloride test), saponins (foam test), steroids (Liebermann Burchard's test), glycosides (Keller-Killiani test), and alkaloids (Dragendorff's test) were analysed as part of the phytochemical screening<sup>24</sup>.

### Green synthesis of silver nanoparticles (AgNPs)

Silver nitrate (AgNO<sub>3</sub>) solutions of 1mM concentrations was prepared. Further, 10 mL of aqueous extract solution was added to 90 mL of 1 mM silver nitrate solution and heated at 60 °C for 4 h until colour shift occurred from green to dark brown which indicates the formation of silver nanoparticles<sup>25</sup>. The green synthesized AgNPs were separated using centrifugation at 15000×g for 20 minutes and filtered using whatman filter paper. The AgNPs were dried at room temperature. The dried AgNPs were collected and calculated the percentage yield of green synthesized AgNPs using formula as given below<sup>26</sup>

$$\% \text{ Yield} = (\text{Weight of dried AgNPs} / \text{Weight of AgNO}_3)$$

## **Characterization of Synthesized Silver Nanoparticles**

### *Ultraviolet visible (UV-Vis) Characterization*

Spectral analysis was performed using a UV-Vis spectrophotometer (UV-1800, Shimadzu, Japan). Spectrum analysis was done between 200 and 800 nm. Different times were used to observe reaction involve in the synthesis of AgNPs by measuring the absorbance using UV-Vis spectrophotometer.

### *Fourier-transform infrared (FT-IR) studies*

The AgNPs were analysed with a Cary 630 FTIR spectrometer (Agilent, USA) to determine the presence of functional groups. The spectral comparison between the extract and AgNPs were performed. The samples were examined from 4000  $\text{cm}^{-1}$  to 600  $\text{cm}^{-1}$  at room temperature.

### *Particle size*

The average particle size and zeta potential of synthesized AgNPs were measured using dynamic light scattering method (Horiba SZ 100, Japan).

### *Transmission electron microscopy (TEM) studies*

The TEM (Jeol/JEM 2100, Jeol, Tokyo, Japan) was utilised to investigate the morphology of AgNPs. One drop of diluted AgNPs dispersion was placed on a copper grid, and another drop of a 2% w/v aqueous solution of phosphotungstate acid was added to improve contrast.

### *Energy diffraction X-ray (EDAX) studies*

The elemental distribution of AgNPs was investigated using energy diffraction X-ray (OXFORD XMX N).

## **Assessment of Antimicrobial activity**

### *Test microorganisms*

The agar well diffusion method was utilised to evaluate the antibacterial potential of the AgNPs. In this investigation, both gram-positive and gram-negative microorganisms were used. The following strains of bacteria were used in this study: *Escherichia coli* (ATCC25922), *Bacillus subtilis* (ATCC23857), *Staphylococcus aureus* (ATCC25923), *Pseudomonas aureginosa* (ATCC15442), and *Bacteroids fragilis* (ATCC23745). Flasks

containing 25 ml of fresh nutrient bath were incubated for 24 h by adding loopful of each bacteria which are maintained in nutrient agar slants.

### *Antimicrobial activity*

Agar-agar and nutrient agar are both dissolved in 100 mL of distilled water and then placed in an autoclave for 30 minutes to create nutrient agar. After letting the fluid harden for a while in Petri dishes, the microbes were distributed using an L-rod. No more than four cavities were drilled into a single plate, and at least a centimetre was left between each one. Using a micro-pipette, samples containing AgNPs were inserted into the wells and incubated for 24 h at 37 °C. The size of the inhibitory zone was then determined. The antibacterial activity was determined by observing the growth of an inhibitory zone around a disc that had been impregnated with plant extract, synthetic AgNPs, and a standard.

### *Minimum inhibitory concentration (MIC)*

The broth dilution method was used to determine the antibacterial effect of AgNPs by observing the development of microbes in the agar broth. The MIC in agar broth was calculated using serial two-fold dilutions of AgNPs in concentrations ranging from 3.12  $\mu\text{g/ml}$  to 25  $\mu\text{g/ml}$  with adjusted bacterial concentration ( $10^8$  CFU/mL, 0.5 McFarland's standard). The streptomycin was taken as standard with the concentration range from 3.12  $\mu\text{g/ml}$  to 25  $\mu\text{g/ml}$ . The control and inoculated broth were incubated at 37 °C for 24 h. The AgNPs concentration at which there was no observable growth in the tubes represented MIC endpoint. The MIC was determined by comparing the clarity and turbidity of the control.

### *Cytotoxicity Studies*

3 mL of PBS were used to reconstitute 15 mg of 3-(4, 5dimethylthiazol-2-yl)-2, 5-diphenyl tetrazolium bromide (MTT) (Sigma, M-5655), after which it was filtered and sterilized. The samples were incubated for 24 h before removing the content in the wells and added 30  $\mu\text{L}$  of MTT solution to each test and control cell well. The plate was shaken gently and incubated for 4 h at 37 °C in 5% CO<sub>2</sub> incubator. The formazan crystal was solubilised by adding 100  $\mu\text{L}$  of DMSO after completing the incubation period. The wells

were mixed properly by pipetting up and down. The absorbance values were obtained with the help of microplate reader at a wavelength of 570 nm. The percentage of viability was determined utilizing the following formula:

$$\% \text{ of viability} = (\text{Mean OD of sample} / \text{Mean OD of Control Group}) \times 100$$

## RESULTS AND DISCUSSION

### Phytochemical Screening

The results of a phytochemical study on *Senna hirsuta* leaf extract are shown in **Table 1**. Results showed the existence of compounds like saponins, tannins, alkaloids, flavonoids, and anthraquinones.

**Table 1:** Phytochemical constituents of *Senna hirsuta* leaf extracts.

Parameters Determined	aqueous extract
Saponins	+
Reducing sugars	+
Tannins	+
Alkaloids	+
Flavonoids	+
Terpenoids	+
Glycosides	+
Phenol	-

### Percentage Yield value

The percentage yield of green synthesized AgNPs was found to be  $31.72 \pm 1.7 \%$ .

### UV-Vis Spectroscopy

10 mL of the aqueous plant extract was combined with 90 mL of the 1 mM aqueous solution of silver nitrate at room temperature. As the reaction progressed, the green leaf extract-silver nitrate solution turned a reddish brown colour (**Fig. 1**). The solution changes from green to a reddish-brown colour as a result of the activation of surface plasmon vibrations in silver nanoparticles<sup>27</sup>. Additionally, AgNPs were synthesized utilizing silver nitrate and periods of exposure to an aqueous leaf extract of *Senna hirsuta*. We used a UV-Vis spectrophotometer to confirm that the  $\lambda_{\text{max}}$  of the synthesized AgNPs lay in the region of 436-446 nm, which is consistent with the results.



**Fig. 1:** Photographs of (A) Plain Extract (B) Silver nanoparticles.

This shift in colour is the first and most obvious indication that nanoparticles have formed, and it is caused by the plasmon resonance phenomenon. Thus, more intense absorption peaks. Since the surface plasmon resonance was excited, the colour and wavelength intensities were boosted. Synthesized AgNPs were observed at different time intervals such as 4 h, 8 h, and 12 h and is depicted in **Fig. 2**. UV-Vis spectra were collected, and it was found that the peak strength rose when the synthesis time for silver nanoparticles was lengthened, showing a broad peak at max at 436-446 nm. In the UV-Vis spectrophotometer, the peak absorption was measured to be at 445 nm. At the end of 12 h of the reaction the absorbance was considerably increased but there was no significant change of lambda value compared to 8 h reaction time. Using leaf extract as a reducing agent, we visually validated that nanoparticle production happens swiftly within 4h<sup>28</sup>.

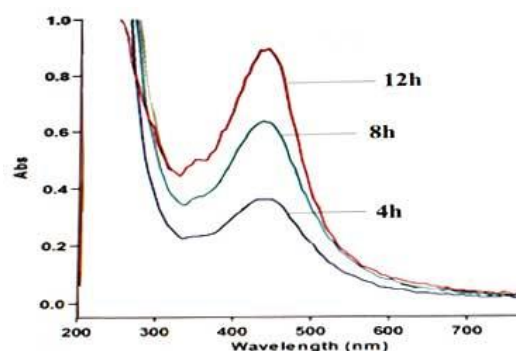


**Fig.2:** UV-Visible spectra illustrating absorbance with different time interval.

### Particle Size

The particle size and polydispersity index of synthesized AgNPs were found 28.3 nm and 0.066 respectively. Size distribution analysis revealed that synthesised AgNPs ranged from 13 nm to 32 nm with low polydispersity index. **Fig. 3** shows the size distribution of the AgNPs. The zeta potential of AgNPs were found -4.4 mV and is shown in **Fig. 4**.

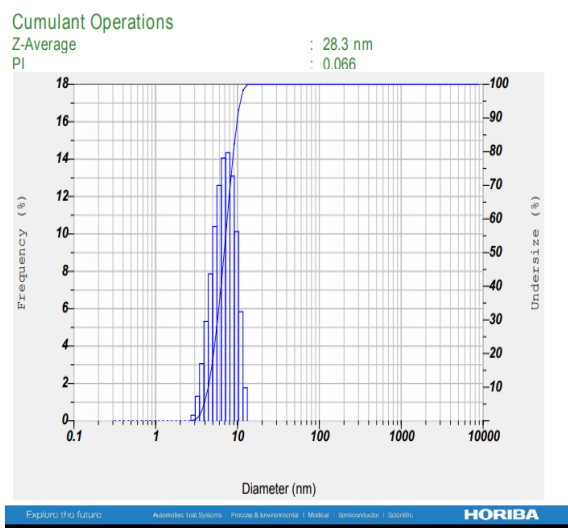


**Fig. 3:** Particle Size of AgNPs.

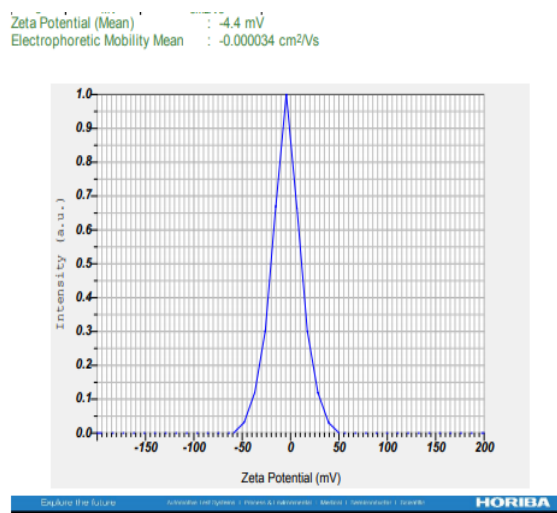


**Fig. 4:** Zeta potential of AgNPs.

### TEM Study

The TEM results showed that the nanoparticles were nanosize and spherical shape (**Fig. 5**). Findings from the transmission electron microscopy investigation corroborated the size obtained from the dynamic light scattering analyses.

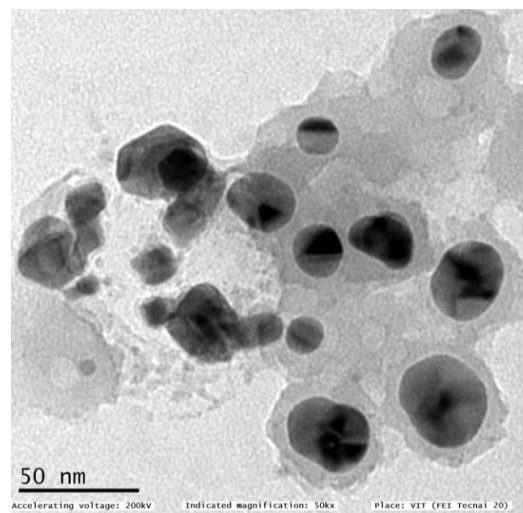


**Fig. 5:** TEM of AgNPs.

### FT-IR Study

Senna hirsuta extract and silver nanoparticles (AgNPs) were both subjected to an FT-IR analysis (**Fig. 6**). The peaks in the FT-IR spectra of AgNPs were found at 3323 cm<sup>-1</sup>, 2113 cm<sup>-1</sup>, and 1636 cm<sup>-1</sup>. The large peak at 3323 cm<sup>-1</sup> was represented for -OH stretching of the phenolic and carboxylic acid groups in senna hirsuta leaf extract. The phytoconstituents of the extract have peaks at 2113 cm<sup>-1</sup> (alkyne group) and 1636 cm<sup>-1</sup> (-CO stretching)<sup>29</sup>. It was revealed that the leaf extract containing Carboxyl (-C=O), Hydroxyl (-OH), and Amine (-NH) groups play a crucial role in the formation of AgNPs. The extract containing high concentrations of polyphenols, triterpenoids, alkaloids, and tannins which possibly played a major role in the formation of AgNPs<sup>30</sup>.

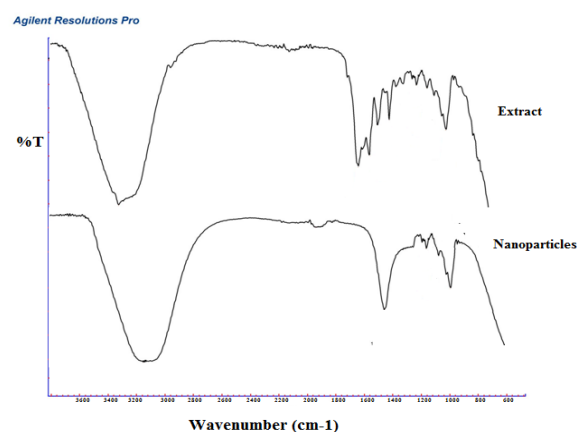


**Fig. 6:** FTIR study of Extract and Nanoparticles (AgNPs).



### EDAX Study

**Fig. 7** shows the EDAX spectra of AgNPs. To be specific, Ag, C, and O were seen in the EDAX of AgNPs. However, AgNO<sub>3</sub> did not show any detectable N signal. Senna hirsuta extract's organic molecules emit carbon and oxygen signals, demonstrating that the extract effectively capping the AgNPs (**Fig. 7**). Silver was detected in the the EDAX spectrum and found strong peak at 3.5 keV. It was observed that, the spectrum containing carbon and oxygen peaks, which were linked to organic components of the leaf extract on the surface of AgNPs and played a major role for reducing and stabilising the AgNPs<sup>31</sup>.

### Antimicrobial Study

The rising prevalence of antibiotic-resistant microbes is one of the biggest obstacles to effectively treating infectious diseases. We therefore set out to develop a method for producing AgNPs using Senna hirsuta leaf extract. The AgNPs showed antimicrobial efficacy against Gram-positive (*S. aureus*) and Gram-negative bacteria (*E. coli*). We examined its antimicrobial efficacy against six distinct bacteria: *E. coli*, *B. subtilis*, *S. aureus*, *P. aureginosa*, and *B. fragilis*. The inhibition zone of nanoparticles was evaluated and compared to that of standard streptomycin. Superior surface area of the silver nanoparticles allowed for more interaction with

the cell wall of bacteria, resulting in potent antibiotic activity<sup>32</sup>. AgNPs typically range in size from 1 to 100 nm. Thus 10-100 nm AgNPs exhibited significant antibacterial action against gram-positive and gram-negative bacteria<sup>33&34</sup>. Antibacterial action of AgNPs is boosted because their small particle size allows them to adhere to the cell wall and easily penetrate the cell of the bacteria. Pure extract, AgNPs, and standard antibiotics were tested to determine their respective zones of inhibition. According to the findings, the inhibitory zone was found more in AgNPs than the extract. **Table 2 and Fig. 8** show the results of the zone of inhibition tests performed on various samples. Due to the electrostatic attraction between the negatively charged microbial cell membranes and the less negatively charged AgNPs causes a significant decrease in the zeta potential of the cell surface upon interaction between the two. Because of the morphological alterations in membrane structure brought on by AgNPs, membrane permeability is disturbed, ultimately resulting in the cell integrity being compromised and the death of the microbe<sup>35</sup>. The outer membrane protein may also interact with AgNPs, causing the formation of complexes with electron donors including phosphorous, oxygen, sulphur, or nitrogen atoms, which can permanently alter the structure of the cell wall<sup>36</sup>.

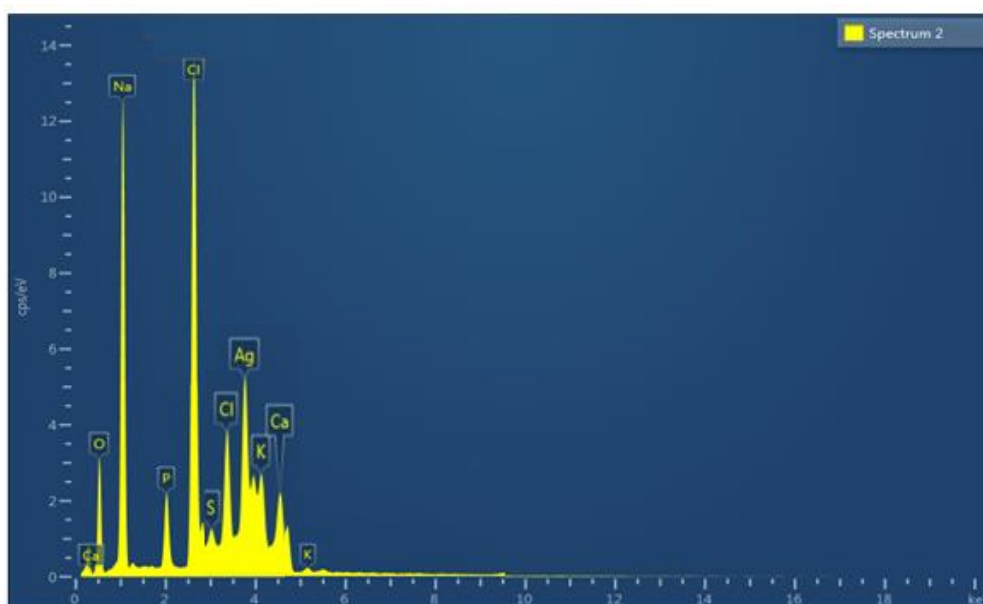


**Fig. 7:** EDAX of AgNPs.

**Table 2:** Zone of inhibition (mm) obtained by the disc diffusion method (Mean  $\pm$  S.D., n=3).

Microorganisms	Zone of inhibition (in mm)		
	Extract	AgNPs	Standard
<i>S. aureus</i>	13 $\pm$ 1.2	18 $\pm$ 0.8	20 $\pm$ 0.6
<i>P. aureginosa</i>	17 $\pm$ 1.7	21 $\pm$ 1.3	26 $\pm$ 0.9
<i>E.coli</i>	20 $\pm$ 1.1	25 $\pm$ 0.7	27 $\pm$ 0.8
<i>B. fragilis</i>	16 $\pm$ 0.8	22 $\pm$ 1.3	24 $\pm$ 0.9
<i>B. subtilis</i>	19 $\pm$ 1.1	24 $\pm$ 0.9	28 $\pm$ 1.1

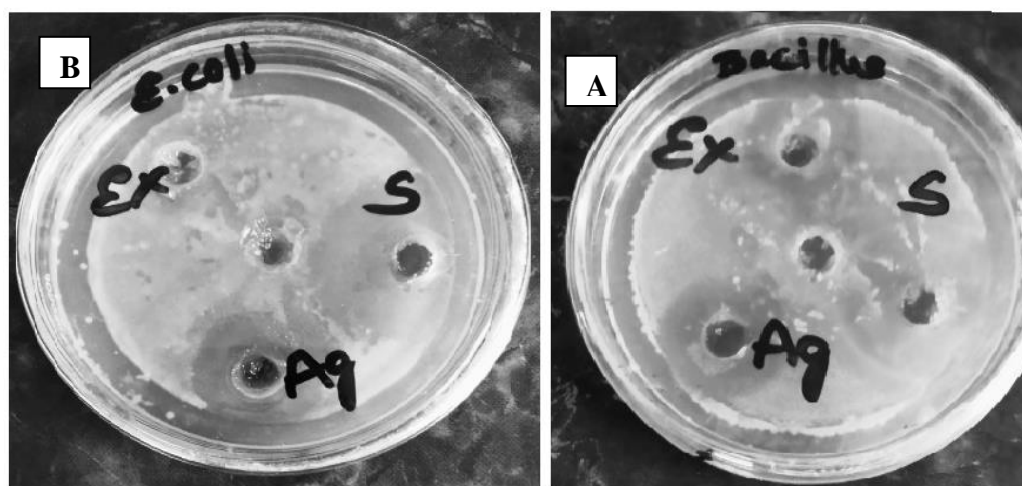


**Fig. 8:** Zone of inhibition of silver nitrate nanoparticles against (A) *E. coli* and (B) *B. subtilis*. (Ag- Silver nitrate nanoparticles; S: Standard; Ex: Extract).

#### Minimum inhibitory concentration (MIC)

Turbidity was detected in the test tubes containing 3.12  $\mu\text{g/ml}$  and 6.25  $\mu\text{g/ml}$  of silver nanoparticles after 24 h of incubation at 37  $^{\circ}\text{C}$ , indicating the growth of bacteria. In contrast, no turbidity was visible at doses of 12.5 and 25  $\mu\text{g/ml}$  demonstrating inhibition of bacterial growth. There was no turbidity observed at a concentration of 6.25  $\mu\text{g/ml}$  and 12.5  $\mu\text{g/ml}$  while using standard drug (streptomycin). Thus, both strptomycin and green synthesized AgNPs were ability to inhibit the microbial growth at low concentrations. According to the results, the bacteria examined could kill at a low AgNPs concentration in a shorter period of time. This might be because gram-negative bacteria have different cell walls compared to gram positive bacteria. gram-negative bacteria have a lipopolysaccharide-containing outer membrane, a thin layer of peptidoglycan, and a cytoplasmic membrane. A space known as the periplasmic space, or periplasm, exists between the outer membrane and the cytoplasmic membrane.

#### Cytotoxicity Studies

The cytotoxicity effect of AgNPs were performed using breast cancer cell lines MCF7. The cytotoxicity of different extract concentrations (concentration ranging from 6.25  $\mu\text{g/mL}$  to 100  $\mu\text{g/mL}$ ) were evaluated and depicted in **Fig. 9**. The cell viability was significantly decrease (below 20 %) while increasing the concentration of biosynthesize AgNPs<sup>37</sup> and is depicted in **Fig. 10**. The minimum detectable cytotoxicity activity and maximum cytotoxicity activity of AgNPs on MCF7 cell line were found 12.54 % (6.25  $\mu\text{g/mL}$ ) and 81.26 % (100  $\mu\text{g/mL}$ ) respectively. The 50% inhibitory concentration ( $\text{IC}_{50}$ ) value was found 28  $\mu\text{g/mL}$ <sup>38</sup>. Due to cancer cells have a tendency to increase the enhanced permeability and retention effect (EPR), more AgNPs enter and concentrate in cancer cells, interact with cancer cells, and ultimately either kill or prevent them from proliferating uncontrollably<sup>39</sup>.

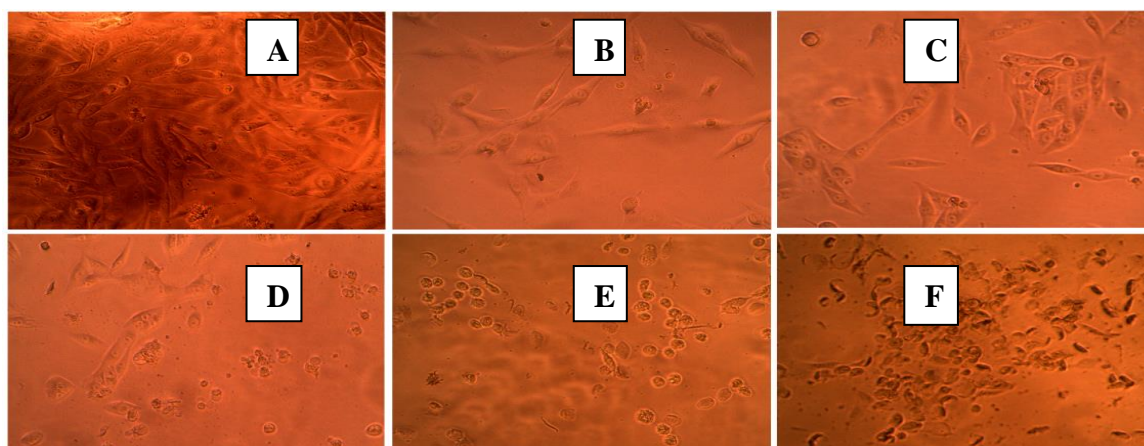


**Fig. 9:** *In vitro* cytotoxicity effect (MTT assay) of (A) Control, (B) 6.25 µg/mL, (C) 12.5 µg/mL, (D) 25 µg/mL, (E) 50 µg/mL, and (F) 100 µg/mL of AgNPs.

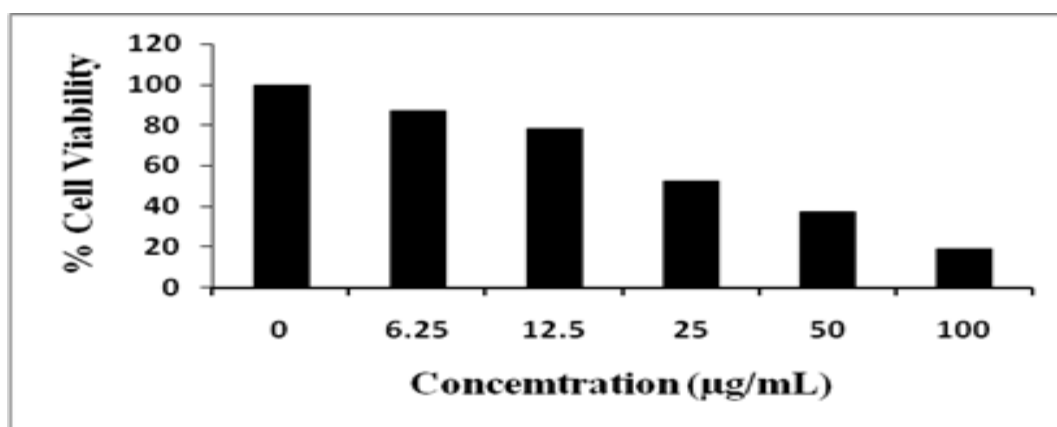


**Fig. 10:** *In vitro* cytotoxicity profile of AgNPs after 24 h incubation at different concentrations.

## Conclusion

*Senna hirsuta* aqueous leaf extract was used to synthesize the silver nanoparticles in a sustainable manner. It was simple, environment friendly and deemed a successful technique for synthesising nanoparticles due to its stability and quick reaction time. The synthesized AgNPs were showed spherical shape. When tested for their antibacterial efficacy against different bacteria, synthesized nanoparticles from *Senna hirsuta* silver showed significantly greater inhibition of gram-negative bacteria than of Gram-positive bacteria. The silver nanoparticles showed better cytotoxicity effect against MCF 7 breast cancer cell lines. The developed AgNPs showed promising carriers for antibacterial and cytotoxicity effects, suggesting a promising direction for further study.

## Conflict of Interests

Authors declare no conflicts of interest

## REFERENCES

1. M. Rai , A.P. Ingle, S. Birla, A. Yadav, and C.A.D. Santos, "Strategic role of selected noble metal nanoparticles in medicine", *Crit Rev Microbiol*, 42(5), 696–719 (2016).
2. K. Niska, E. Zielinska, M.W. Radomski, and I. Inkielewicz-Stepniak, "Metal nanoparticles in dermatology and cosmetology: interactions with human skin cells", *Chem Biol Interact*, 295, 38–51 (2018).
3. H.P. Borase, B.K. Salunke, R.B. Salunkhe, C.D. Patil, J.E. Hallsworth, B.S. Kim, and S.V. Patil, "Plant extract: a promising biomatrix for eco-friendly, controlled



- synthesis of silver nanoparticles", *Appl Biochem Biotechnol*, 173, 1–29 (2014).
4. A.K. Mittal, J. Bhaumik, S. Kumar, and U.C. Banerjee, "Biosynthesis of silver nanoparticles: elucidation of prospective mechanism and therapeutic potential", *J Colloid Interface Sci*, 415, 39–47 (2014).
  5. B. Pannerselvam, M.K.D. Jothinathan, M. Rajenderan, P. Perumal, K.P. Thangavelu, H.J. Kim, V. Singh, and S.K. Rangarajulu, "An *in vitro* study on the burn wound healing activity of cotton fabrics incorporated with photosynthesized silver nanoparticles in male wistar albino rats", *Eur J Pharm Sci*, 100, 187–196 (2017).
  6. A.S. Takamiya, D.R. Monteiro, D.G. Bernabe, L.F. Gorup, E.R. Camargo, J.E. Gomes-Filho, S.H.P. Oliveira, and D.B. Barbosa, "*In vitro* and *in vivo* toxicity evaluation of colloidal silver nanoparticles used in endodontic treatments", *J Endod*, 42(6), 953–960 (2016).
  7. K. Jadhav, D. Dhamecha, D. Bhattacharya, and M. Patil, "Green and eco friendly synthesis of silver nanoparticles: characterization, biocompatibility studies and gel formulation for treatment of infections in burns", *J Photochem Photobiol B Biol*, 155, 109–115 (2016).
  8. L.C. Savery, R. Vinas, A.M. Nagy, P. Pradeep, S.J. Merrill, A.M. Hood, S.G. Malghan, P.L. Goering, and R.P. Brown, "Deriving a provisional tolerable intake for intravenous exposure to silver nanoparticles released from medical devices", *Regul Toxicol Pharmacol*, 85, 108–118 (2017).
  9. R. Jayaraman, P. Sampathi, N.N. Palei, A. Balaji, S.A. Shyam, B.C. Mohanta BC, and V.R. Palanimuthu, "Green synthesis, characterization and antiepileptic activity of herbal nanoparticles of *Mimusops elengi* in mice", *Nano Biomed Eng*, 14(4), 295–301 (2022).
  10. S.K. Nandi, A. Shivaram, S. Bose, and A. Bandyopadhyay, "Silver nanoparticle deposited implants to treat osteomyelitis", *J Biomed Mater Res B Appl*, 106(3), 1073–1083 (2016).
  11. A.S. Mohd, S. Sunitha, A.S. Mohmmad, S.K.K. Pasha, and D. Choi, "An overview of antimicrobial and anticancer potential of silver nanoparticles", *J King Saud Univ Sci*, 34(2), 101791 (2022).
  12. A.C. Gomathi, R.S.R. Xavier, S.A. Mohammed, and S. Rajeshkumar, "Anticancer activity of silver nanoparticles synthesized using aqueous fruit shell extract of *Tamarindus indica* on MCF-7 human breast cancer cell line", *J Drug Delivery Sci Technol*, 55, 101376 (2020).
  13. C. Rajkuberan, S. Prabukumar, G. Sathishkumar, A. Wilson, K. Ravindran, and S. Sivaramakrishnan, "Facile synthesis of silver nanoparticles using *Euphorbia antiquorum* L. latex extract and evaluation of their biomedical perspectives as anticancer agents", *J Saudi Chem Soc*, 21(8), 911-919 (2017).
  14. H. Wang, X. Qiao, J. Chen, and S. Ding, "Preparation of silver nanoparticles by chemical reduction method", *Colloids Surf A Physicochem Eng Asp*, 256(2-3), 111-115 (2005).
  15. O.D. Petrucci, R.J. Hilton, J.K. Farrer, and R.K. Watt, "A ferritin photochemical synthesis of monodispersed silver nanoparticles that possess antimicrobial properties", *J Nanomater*, 2019, 1-8 (2019).
  16. R.A. Khaydarov, R.R. Khaydarov, O. Gapurova, Y. Estrin, and T. Scheper, "Electrochemical method for the synthesis of silver nanoparticles", *J Nanoparticle Res*, 11, 1193-1200 (2009).
  17. M.V. Roldan, N. Pellegrini, and O. Sanctis, "Electrochemical method for Ag-PEG nanoparticles synthesis", *J Nanoparticles*, 2013, 1-7 (2013).
  18. S. Iravani, H. Korbekandi, S.V. Mirmohammadi, and B. Zolfaghari, "Synthesis of silver nanoparticles: Chemical, physical and biological methods", *Res Pharm Sci*, 9(6), 385-406 (2014).
  19. V.L. Das, R. Thomas, R.T. Varghese, E.V. Soniya, J. Mathew, and E.K. Radhakrishnan, "Extracellular synthesis of silver nanoparticles by the *Bacillus* strain CS 11 isolated from industrialized area", *3 Biotech*, 4(2), 121-126 (2014).
  20. P. Logeswari, S. Silambarasan, and J. Abraham, "Synthesis of silver

- nanoparticles using plants extract and analysis of their antimicrobial property", *J Saudi Chem Soc*, 19(3), 311-317 (2015).
21. S. Pirtarighat, M. Ghannadnia, and S. Baghshahi, "Green synthesis of silver nanoparticles using the plant extract of *Salvia spinosa* grown in vitro and their antibacterial activity assessment", *J Nanostructure Chem*, 9, 1-9 (2019).
  22. K.Gudikandula, P. Vadapally, and M.A. Charya, "Biogenic synthesis of silver nanoparticles from white rot Fungi: Their characterization and antibacterial studies", *Open Nano*, 2, 64-78 (2017).
  23. S. Ahmed, M. Saifullah Ahmad, B.L. Swami, and S. Ikram, "Synthesis of silver nanoparticles using *Azadirachta indica* aqueous leaf extract", *J Radiat Res Appl Sci*, 9(1), 1-7 (2016).
  24. M. Sabapati, N.N. Palei, C.K. Ashok kumar, and M. Rabindra Babu, "Solid lipid nanoparticles of *Annona muricata* fruit extract: formulation, optimization and in vitro cytotoxicity studies", *Drug Dev Ind Pharm*, 45(4), 577-586 (2019).
  25. Hemlata, P.R. Meena, A.P. Singh, and K.K. Tejavath, "Biosynthesis of silver nanoparticles using *Cucumis prophetarum* aqueous leaf extract and their antibacterial and antiproliferative activity against cancer cell lines", *ACS Omega*, 5(10), 5520-5528 (2020).
  26. R. Sood and D.S. Chopra, "Improved yield of green synthesized crystalline silver nanoparticles with potential antioxidant activity", *Int Res J Pharm*, 8, 100-104 (2017).
  27. R. Veerasamy, T.Z. Xin, S. Gunasagaran, T.F.W. Xiang, E.F.C. Yang, N. Jeyakumar, and S.A. Dhanaraj, "Biosynthesis of silver nanoparticles using mangosteen leaf extract and evaluation of their antimicrobial activities", *J Saudi Chem Soc*, 15(2), 113-120 (2011).
  28. E.R. Carmona, N. Benito, T. Plaza, and G. Recio-Sanchez, "Green synthesis of silver nanoparticles by using leaf extracts from the endemic *Buddleja globosa* hope", *Green Chem Lett Rev*, 10(4), 250-256 (2017).
  29. P. Banerjee, M. Satapathy, A. Mukhopahayay, and P. Das, "Leaf extract mediated green synthesis of silver nanoparticles from widely available Indian plants: Synthesis, characterization, antimicrobial property and toxicity analysis", *Bioresour Bioprocess*, 1, 3 (2014).
  30. P.R. Hemlata, A.P. Meena, Singh, and K.K. Tejavath, "Biosynthesis of Silver Nanoparticles Using *Cucumis prophetarum* Aqueous Leaf Extract and Their Antibacterial and Antiproliferative Activity Against Cancer Cell Lines", *ACS Omega*, 5(10), 5520-5528 (2020).
  31. U.B. Jagtap, and V.A. Bapat, "Green synthesis of silver nanoparticles using *Artocarpus heterophyllus* Lam. seed extract and its antibacterial activity", *Ind Crops Prod*, 46, 132-137 (2013).
  32. X.F. Zhang, Z.G. Liu, W. Shen, and S. Gurunathan, "Silver nanoparticles: synthesis, characterization, properties, applications, and therapeutic approaches", *Int J Mol Sci*, 17(9), E1534 (2016).
  33. J.R. Morones, J.L. Elechiguerra, A. Camacho, K. Holt, J.B. Kouri, J.T. Ramirez, and M.J. Yacaman, "The bactericidal effect of silver nanoparticles", *Nanotechnology*, 16, 2346-2353 (2005).
  34. Y.Y. Loo, Y. Rukayadi, M.A.R. Nor-Khaizura, C.H. Kuan, B.W. Chieng, M. Nishibuchi, and S. Radu, "In vitro antimicrobial activity of green synthesized silver nanoparticles against selected gram-negative food borne pathogens", *Front Microbiol*, 9, 1555 (2016).



## نشرة العلوم الصيدلانية جامعة أسيوط



### تأثير السمية الخلوية و التأثير المضاد للميكروبات في المختبر لجسيمات الفضة النانوية الخضراء المركبة باستخدام مستخلص الأوراق المائية من سينا هيرسوتا

ناراهاري ن. بالي<sup>1\*</sup> - م. ب. البرلمان بوفانا<sup>2</sup> - ر. جايارامان<sup>3</sup> - أرجيا كوسوم دار<sup>4</sup>

<sup>1</sup>معهد أميتي للصيدلة، جامعة أميتي أوتار براديش، حرم لكانو، الهند

<sup>2</sup>كلية سري فيديانيكثان للصيدلة، تيروباتي، أندرا براديش، الهند

<sup>3</sup>كلية الصيدلة شري فينكاتيشوارا، أريور، بونديشيري، الهند

<sup>4</sup>كلية الصيدلة، جامعة نيوتيا، ساريشا، ولاية البنغال الغربية، الهند

في هذه الدراسة، قمنا بإعداد جسيمات الفضة النانوية (AgNPs) باستخدام مستخلص أوراق سينا هيرسوتا المائي. تم توصيف AgNPs باستخدام مقياس الطيف الضوئي المرئي للأشعة فوق البنفسجية، وحجم الجسيمات، وجهد زيتا، والأشعة السينية لحيود الطاقة (EDAX)، والأشعة تحت الحمراء لتحويل فورييه (FTIR)، والمجهر الإلكتروني النافذ (TEM) وتحديد تأثير السمية الخلوية و التأثير المضاد للبكتيريا. تم إجراء التحليل الطيفي المرئي للأشعة فوق البنفسجية لمستخلص أوراق سينا هيرسوتا الذي تم تصنيعه في جسيمات الفضة النانوية على فترات زمنية مختلفة. لوحظت الذروة ( $\lambda_{max}$ ) عند 436-446 نانومتر وكانت واسعة. وجد أن حجم الجسيمات كان 28,3 نانومتر وقيمة جهد زيتا كان -4,4 مللي فولت أظهرت جسيمات الفضة النانوية نشاطا فعالا مضادا للميكروبات بسبب مساحة سطحها الكبيرة، مما يسمح باتصال أقوى مع جدار الخلية من البكتيريا. أظهرت السمية الخلوية في المختبر أن الجسيمات النانوية لها نشاط سمية خلوية بارز ضد خطوط خلايا MCF7.